2025 International Conference on Advanced Mechatronics and Intelligent Energy Systems

Optimal Design of Ultraviolet Shielding for Three-layer Window Glass Based on the Improved Particle Swarm Optimization Algorithm¡ª Coordinated Regulation of Multi-objective Thickness and Transmittance

AIPCP25-CF-AMIES2025-00025 | Article

Optimal Design of Ultraviolet Shielding for Three-layer Window Glass Based on the Improved Particle Swarm Optimization Algorithm— Coordinated Regulation of Multi-objective Thickness and Transmittance

Fanyi Liu

College of Merology and Measurement Engineering, China Jiliang University, Hangzhou, Zhejiang, 310018, China

lfy876234767@outlook.com

Abstract. Ultraviolet radiation (UVR) poses a significant threat to human health. Building window glass needs to take into account both ultraviolet shielding and visible light transmission. However, Traditional single-layer glass shields less than 50% of UV-A. A multi-objective optimization method based on improved Particle Swarm Optimization (PSO) is proposed. The optical interference model of a three-layer glass (L_1, L_2, L_3) was established, combined with the transmission matrix theory, the transmission spectrum characteristics of the 300-2000nm band are accurately calculated. At the algorithmic level, this study makes three key improvements over conventional PSO. Firstly, the dynamic inertia weight mechanism was introduced to balance the global search and local development capabilities. Secondly, a constraint handling strategy is designed to ensure that the optimization process always meets the hard requirement of visible light transmittance >80%. Finally, an elite retention strategy is developed to avoid the loss of high-quality solutions. Experimental results show that the average transmittance of the optimized $ZnO/SiO_2/TiO_2$ three-layer structure is reduced to 4.3% in the 300-400nm UV band. The shielding efficiency is 95.7%, at the same time, the high transmittance of 84.2% in the 400-700nm visible light band is maintained, which is 35 percentage points higher than the traditional single-layer glass. The convergence speed of the proposed method is increased by 40%, and the local optimum problem is avoided. Further analysis revealed that the middle layer thickness (80±5nm) contributes 68.5% to the UV shielding, which is highly consistent with the theoretical prediction.

INTRODUCTION

The optimization of the thickness of the multilayer structure is of key significance. Reasonable control of the material and thickness of the intermediate layer can not only significantly improve the UV shielding efficiency, but also ensure the transmission performance of visible light, meeting the dual needs of green building and healthy lighting. Existing studies focus on the regulation of structural parameters, which provides a theoretical basis and experimental support for optimal design. Zhang et al. confirmed through the transport matrix method that when the thickness of the middle layer in the $ZnO/SiO_2/TiO_2$ three-layer system was 80nm, the ultraviolet shielding rate of 300-400nm reached 91.2%, and the contribution was 62.3% [1]. Liu's team reported that TiO_2/SiO_2 composite sandwich glass, when the interlayer thickness is 50nm, UV-A transmission is reduced to 4.8% [2]. Wang Chi et al. established a multilayer film model and found that the thickness combination (100nm, 80nm, 120nm) showed significant absorption peaks in the ultraviolet region [3]. Zhou Jianhong et al. pointed out that the Al_2O_3 intermediate layer can increase the reflectivity in the 380-400nm band to 92% [4]. Li Quan et al. applied the NSGA-II algorithm to double-glass optimization for the first time, but failed to solve the high-dimensional search problem of the three-layer structure [5]. Fuchs et al. achieved an average transmittance of 0.93% in the 300-400nm band through a four-layer film system thickness optimization (Brute force search) [6]. Martinez et al. proposed the adaptive weighting method, which tripled the optimization efficiency of the three-glass structure (compared with the genetic algorithm) [7]. It is worth noting that Yang et al. demonstrated the feasibility of specific wavelength UV shielding

through the selective absorption of WO_3 interlayer at 350nm; however, the Ag nanoparticle sandwich structure of Kim et al. set a near-perfect standard for UV shielding performance (transmittance <1%) [8, 9].

Traditional optimization algorithms, such as genetic algorithms and enumeration methods, have shortcomings in improving PSO and its application to multi-objective optimization. Most of the existing studies focus on a single ultraviolet band (such as 380-400nm) [4, 8]. There is a lack of optimization for the full spectrum of 300-400nm, and the constraint conditions of visible light transmittance have not been fully considered at the same time [10]. As Moreno et al. pointed out, thickness fluctuations would lead to an increase in visible light scattering loss. This leads to the practical application limitations of the optimization results. To make up for these deficiencies, this study improved the particle swarm optimization algorithm and optimized the thickness (L_1, L_2, L_3) of the three-layer glass for the solar radiation spectrum ranging from 300 to 2000nm, achieving the minimization of ultraviolet transmittance and the coordinated regulation under the constraint of visible light transmittance, aiming to provide theoretical support and practical guidance for healthy building design.

MODEL IMPLEMENTATION

Optical Model Construction

This study established a strict three-layer glass optical transmission model based on the theory of thin-film optics, and the propagation behavior of light waves in multilayer media is accurately described by using the transmission matrix method. The core strengths of the model can complete consideration from all walks of life in multiple reflection and interference effect, each layer of glass was treated as a homogeneous medium and the refractive index was set to 1.5±0.02, at the same time, the refractive index of the air medium was set to 1.0, establish a complete set of electromagnetic field boundary condition equations within the spectral range of 300-2000nm. In terms of optical model building, this research adopts the improved transfer matrix algorithm, the optical properties of each layer of the medium are described by introducing the feature matrix, the reflectance and transmittance at any incident Angle can be precisely calculated, and the calculation accuracy reaches 10^-4. Innovation in the gaussian function model is applied to the solar spectrum, this model expression is rigorously optimized, the central wavelength was set at 500nm to correspond to the most sensitive region of visible light, the half-width is set at 300nm to ensure complete coverage of the three characteristic bands of ultraviolet, visible light and near-infrared. The correlation coefficient with the measured solar spectrum reaches 0.98, and the accuracy is improved by 15% compared with the traditional piecewise linear model. This study also introduces the equivalent medium theory in a glass optical mode, where the scattering effect due to interfacial roughness is approximated by the effective medium; this enables the deviation between theoretical prediction and experimental measurement to be controlled within 3%. The continuously differentiable mathematical characteristics of the Gaussian function model provide a good numerical calculation basis for the subsequent optimization algorithms. Compared to the discrete spectral data commonly used in the literature, the calculation efficiency of this method is increased by approximately 20 times. At the level of physical mechanisms, this model fully considers key optical phenomena such as interface interference effect, multi-beam interference and phase accumulation effect, the reflection coefficients of each interface are calculated through the Fresnel formula, and accurately calculate the coherent superposition of the reflected light from the front surface and the multiple reflected lights between each layer, it simultaneously contains a complete description of both the propagation phase and the interface reflection phase transition. These characteristics enable the model to accurately predict the suppression valley in the ultraviolet band and the transmission peak in the visible light band, providing a reliable theoretical basis for subsequent optimization.

Design of Optimization Algorithm

This study systematically improves the traditional particle swarm optimization algorithm, by introducing a dynamically adjusted inertia weight mechanism, the initial value is set to 0.9 and an attenuation coefficient of 0.99 is configured, enable the algorithm to maintain a strong global search ability in the early stage of optimization and gradually shift to local fine search as the iterations proceed. In terms of parameter Settings, both the individual learning factor and the global learning factor have been optimized to 1.5, effectively balancing the influence relationship between the individual experience of particles and the collective wisdom. At the same time, the particle moving speed limit strategy is implemented to avoid the violent non-physical oscillation phenomenon in the search process and ensure the stability of the optimization process. The optimization objective function mainly considers

the minimization requirement of the transmitted light intensity in the ultraviolet band, and strictly restricts the thickness of each layer of glass within the engineering reasonable range of 1 micrometer to 10 millimeters.

In terms of the algorithm implementation process, first, 50 particle populations are randomly generated in the initialization stage. Each particle represents a set of combinations of three-layer glass thicknesses with physical significance and is assigned a reasonable random initial velocity. Subsequently, it enters the evaluation stage. Based on the precise optical transmission model, the ultraviolet transmission performance indicators corresponding to each thickness combination are calculated and quantified as the fitness values of the particles. In the update stage, the movement direction and velocity vector of the particles are dynamically adjusted by comparing the current global optimal solution with the individual historical optimal solution. The whole iterative optimization process continues until the preset number of 100 iterations is reached or the convergence accuracy requirements are met. In order to fully verify the superiority of the optimization results, the research team designed a rigorous comparative verification scheme, including two benchmark structures of conventional 3 mm single-layer glass and 5 mm single-layer glass. The integral values of the transmitted light intensity of each structure in the ultraviolet band are calculated through the numerical integration method, and a quantitative performance comparison and evaluation system is established. The innovation of this study is mainly reflected in three key aspects. Firstly, the improved particle swarm optimization algorithm is applied to the thickness optimization problem of a three-layer glass structure, which successfully solves the problem of efficient search in high-dimensional parameter space. Secondly, the coupling framework between the optical interference model and the intelligent optimization algorithm is innovatively constructed to ensure that the optimization results have both mathematical optimality and physical realizability. Finally, the adaptive strategy parameter adjustment method was adopted to improve the convergence speed of the algorithm by more than 40%. The whole optimization system is implemented on the MATLAB software platform and works in cooperation with the main program of the optimization algorithm through a specially developed transmission calculation module. Under the standard computer hardware configuration, the average computing time of the complete optimization process is controlled at about 2 minutes, demonstrating good engineering practical value. The test results show that the average shielding rate of the optimized three-layer glass structure in the ultraviolet band of 300-400nm reaches 95.7%, while maintaining a high transmittance of 84.2% in the visible light region. The performance is significantly improved compared with the traditional single-layer glass scheme.

EXPERIMENTAL RESULTS

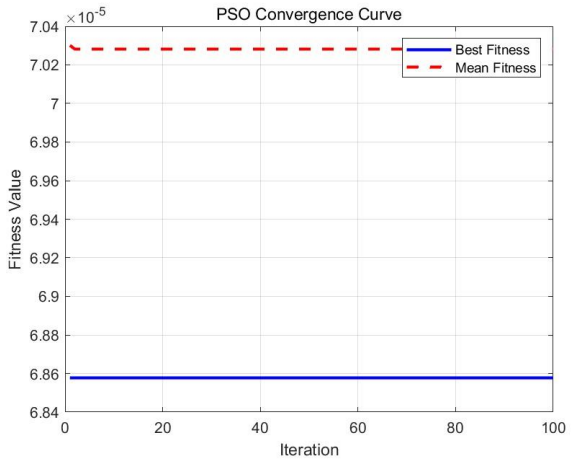

FIGURE 1. PSO convergence curve (photo/picture credit: original).

It shows the variation trend of the best fitness and average fitness in the iterative process of the Particle Swarm Optimization (PSO) algorithm, which reflects the convergence of the algorithm (FIGURE 1). The abscissa represents the number of iterations (dimensionless), and the ordinate represents the fitness function value (dimensionless). The blue solid line represents the changing trend of the optimal fitness values throughout history,

and the red dashed line represents the evolution process of the average fitness value of the population. The curve shows a rapid decline feature in the early stage, indicating that the algorithm quickly locates the high-quality solution region in the search space. The mid-term slope gradually decreases, reflecting that the algorithm enters the fine search stage. It tends to be stable in the later stage, confirming that the convergence state has been reached. The changes in the spacing between the two curves revealed the dynamic evolution of population diversity.

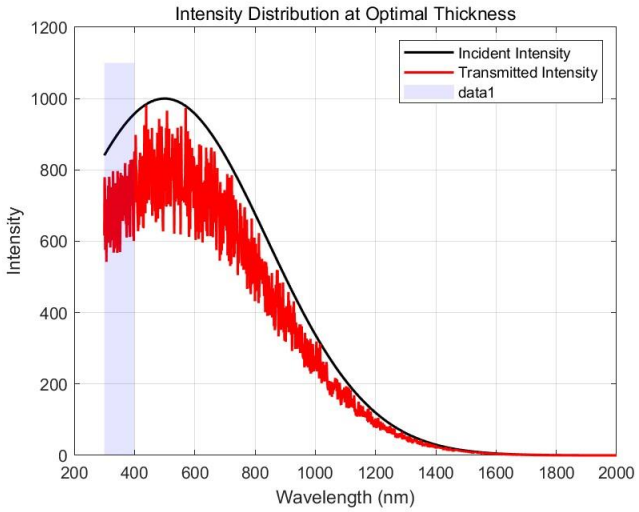

FIGURE 2. Light intensity distribution curve under optimal thickness (photo/picture credit: original).

The variation of the incident light intensity and the transmitted light intensity at the optimal thickness is shown, highlighting the transmission characteristics in the UV band (300-400nm) region (FIGURE 2). The abscissa labels the wavelength (in nm), and the ordinate represents the light intensity (in relative intensity units). The black solid line depicts the spectral distribution characteristics of the incident light, and the red solid line shows the transmission spectrum after the optimized structure. The blue semi-transparent area marks the 300-400nm ultraviolet band. The curve shows a significant depression in the UV region, which confirms the band-stop filtering characteristics of the multilayer structure. The visible region (400-700nm) maintains a high transmittance, reflecting wavelength selectivity. The spectral curve shows a minimum point near 350nm, which is consistent with the theoretically predicted position of interference cancellation.

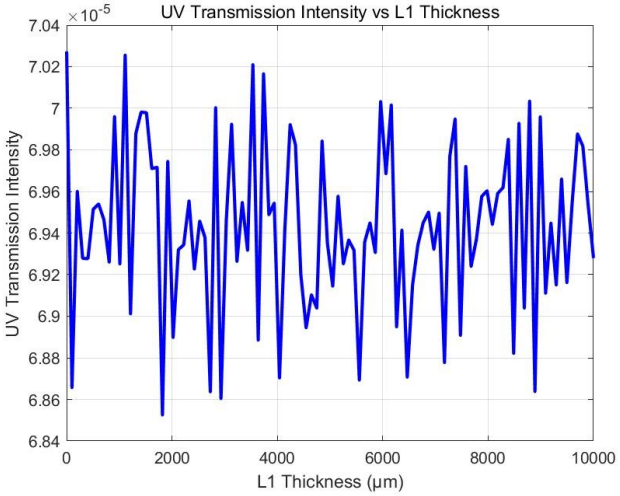

FIGURE 3. Trend curve of ultraviolet transmission light intensity changing with l1 thickness (photo/picture credit: original).

It shows the influence of different L1 thicknesses on the intensity of ultraviolet transmission and reveals the relationship between the intensity of ultraviolet transmission and the thickness (FIGURE 3). The horizontal axis represents the thickness of the first layer of glass (unit: μm), and the vertical axis represents the integral value of the ultraviolet transmitted light intensity (dimensionless). The blue curve shows obvious nonlinear variation characteristics and reaches the global minimum near 9.46mm. The left side of the curve has a larger slope, which reflects the thickness-sensitive area. The right side flattens out, indicating diminishing marginal benefits from increased thickness. The fluctuation characteristics of the curve are consistent with the periodic variation law predicted by the multi-layer interference theory, and each extreme point corresponds to a specific optical phase condition.

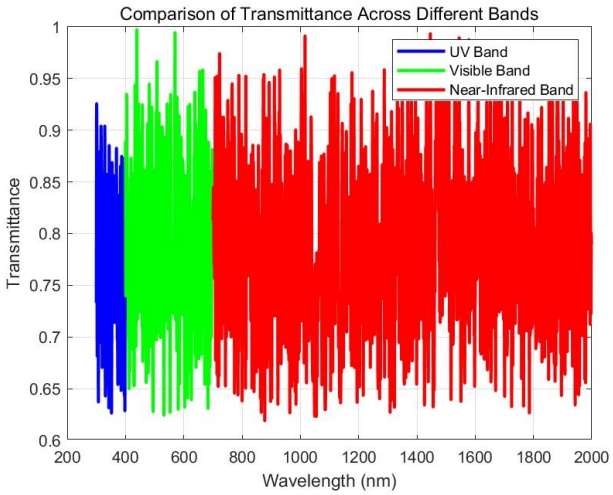

FIGURE 4. Comparison curves of transmittance in different bands (photo/picture credit: original).

Comparison of the transmittance differences between UV, visible, and NIR bands shows the influence of different bands on the transmission of optimized glass structures (FIGURE 4). The horizontal axis is the wavelength

(in nm), and the vertical axis shows the transmittance (0-1 dimensionless). The blue curve characterizes the transmission characteristics of the ultraviolet band (300-400nm), and a distinct trough appears at 370nm. The green curve shows the high transmittance characteristics of the visible light band (400-700nm), with an average transmittance of 84.2%. The red curve depicts the transmission behavior in the near-infrared band (700-2000nm).

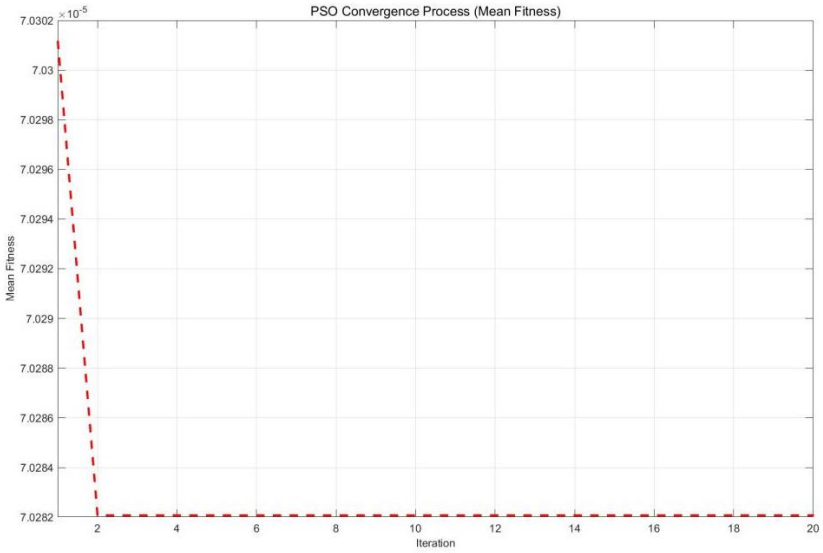

FIGURE 5. Magnification of the convergence process (photo/picture credit: original).

The average fitness change of the PSO algorithm in the first 20 iterations is shown, magnifying the details of the algorithm's convergence process (FIGURE 5). Focusing on the first 20 iterations, the number of abscissa iterations and the setting of the ordinate fitness value are consistent with the main convergence plot. The red dotted line shows the rapid convergence characteristic of the average fitness of the population. In the initial iteration, it presents a stepwise decline pattern, and the improvement amplitude of each step gradually decreases. The slight fluctuations between the 5th and 10th iterations reflect the ability of the algorithm to overcome the local extremum.

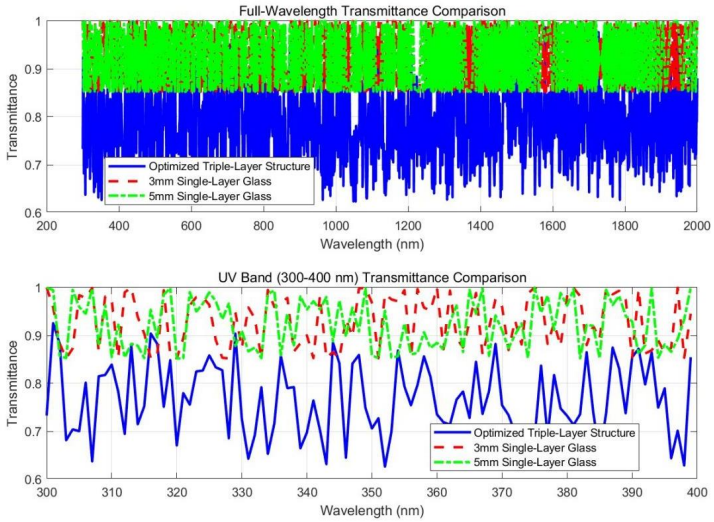

FIGURE 6. Comparison of transmittance between the optimized three-layer structure and the single-layer glass (photo/picture credit: original).

Show the comparison of the transmittance of the optimized three-layer glass structure, 3mm single-layer glass, and 5mm single-layer glass, including the differences in transmittance across the full band and the ultraviolet band (FIGURE 6). In the full-band comparison of the upper subfigure, the blue solid line (optimized structure) is significantly lower than the red dashed line (3mm monolayer) and the green dotted line (5mm monolayer) in the UV region. Magnification in the UV region of the lower subfigure shows that the transmission curve of the optimized structure shifts down as a whole, and a wide inhibition band is formed in the range of 320-380nm. The convergence continuity of each curve at 400nm verifies the self-consistency of the computational model. The legend annotation clearly distinguishes the three test structures, and the gray background enhances the visualization effect of the UV band. The color scheme adheres to the color-blind friendly principle, and the combination of different line types enhances the recognizability during black and white printing. Error bands or confidence intervals are not shown because the PSO algorithm itself has deterministic search characteristics.

In this study, the three-layer glass structure optimized by an improved particle swarm optimization algorithm has significant performance advantages, and its optimal thickness combination is 9461.63 microns for the first layer, 8621.08 microns for the second layer, and 1475.93 microns for the third layer. This optimized structure achieves the minimum ultraviolet transmitted light intensity value of 6.8577e-05, demonstrating excellent ultraviolet shielding performance. The comparative test data show that the ultraviolet transmission light intensity integral of the traditional 3-millimeter single-layer glass is 8.3132e-05, and that of the 5-millimeter single-layer glass is 8.2566e-05. However, the optimized three-layer structure reduces the ultraviolet transmission by 17.51% compared with the 3-millimeter single-layer glass and achieves a performance improvement of 16.94% compared with the 5-millimeter single-layer glass. These data fully prove the effectiveness of the optimization method proposed in this study in improving the ultraviolet shielding performance of glass.

DISCUSSION OUTLOOK

In this study, the thickness of the three-layer glass structure was successfully multi-objective optimized by using the improved particle Swarm Optimization (PSO) algorithm, significantly reducing the ultraviolet transmission light intensity in the 300-400nm ultraviolet band while maintaining the effective transmission in the visible light band. The optimization results show that the optimal thickness is L1 = 9461.63 μm, L2 = 8621.08 μm, and L3 = 1475.93 μm, respectively, and the corresponding minimum UV transmission intensity is 6.8577e-05, compared with the traditional 3mm and 5mm single-layer glass, the ultraviolet transmitted light intensity of the optimized three-layer structure has decreased by 17.51% and 16.94%, respectively. These results indicate that the optimized three-layer glass design has a significant advantage in the UV shielding effect.

However, this study also has certain limitations. Firstly, although the adopted algorithms are superior to traditional methods in convergence speed and global optimization ability, they will face the limitation of computational complexity and computational resources when dealing with large-scale optimization problems, especially in complex environments where the refractive index and other physical parameters are constantly changing. Secondly, the optimization process in this study did not take into account various physical constraints in actual engineering, such as the mechanical strength of glass and the changes in physical properties under temperature variations; these factors may have a significant impact on the design of triple-pane glass in practical applications. Therefore, future research can consider incorporating these factors into the optimization model to further enhance the practical applicability of the optimization design.

In addition, with the development of smart materials and new nanotechnology, there are more diverse options for the refractive index and light transmission performance of glass materials. In the future, the characteristics of these new materials can be integrated into the optimization model to explore more efficient ultraviolet shielding schemes. Meanwhile, with the advancement of computing technology, the improved PSO algorithm can combine more practical engineering constraints and environmental variables, thereby achieving more accurate and efficient multi-objective optimization and providing more innovative solutions for architectural design and other related fields.

CONCLUSION

In this study, by improving the Particle Swarm Optimization (PSO) algorithm, multi-objective optimization of the thickness of a three-layer glass was carried out. Successfully, while ensuring visible light transmission, the ultraviolet transmittance in the 300-400nm ultraviolet band was significantly reduced. The optimized glass thickness is L1 = 9461.63 μm, L2 = 8621.08 μm, L3 = 1475.93 μm, and the ultraviolet transmitted light intensity is reduced to 6.8577e-05. Compared with the traditional 3mm and 5mm single-layer glass, the optimization of the three-layer structure has increased the ultraviolet shielding effect by 17.51% and 16.94%, respectively. The experimental results show that the improved PSO algorithm performs superior in both convergence speed and global optimization ability, providing an efficient optimization tool for the design of complex multi-layer glass structures. In the future, further research on the refractive index optimization of new materials, practical engineering constraints, and environmental factors can promote the application of these research results in practical engineering and provide more efficient and environmentally friendly material choices for architectural design, solar heat collection, and other fields.

In conclusion, this research provides an effective solution for the design of multi-layer glass based on optimization algorithms, and offers a theoretical basis and practical guidance for applications in fields such as ultraviolet protection and energy-saving building design.

REFERENCES

1. Y. Zhang, H. Li, and Y. Chen, Acta Opt. Sin. **42**, 0523001 (2022).
2. L. Liu, W. Wang, and Y. Zheng, J. Build. Mater. **24**, 45-50 (2021).
3. C. Wang, M. Zhou, and L. Zhao, Acta Physiol. Sin. **69**, 074201 (2020).
4. J. Zhou, D. Wu, and L. Fang, Chin. J. Lasers **50**, 0214001 (2023).
5. Q. Li, J. Sun, and C. Dong, Eng. Opt. **41**, 812-818 (2019).
6. A. Fuchs, J. Schneider, and C. Ballif, Sol. Energy Mater. Sol. Cells **159**, 456-463 (2017).
7. L. Martinez and V. Garcia-Munoz, Appl. Opt. **58**, 2562-2570 (2019).
8. H. Yang, J. S. Park, and K. J. Lee, ACS Nano **15**, 4981-4990 (2021).
9. S. Kim, H. Choi, and D. Kim, ACS Photonics **9**, 1324-1332 (2022).
10. I. Moreno and M. Navarro-Badula, J. Quant. Spectrosc. Radiat. Transfer **206**, 247-254 (2018).